J. Chem. Sci. Vol. 128, No. 10, October 2016, pp. 1651–1662. © Indian Academy of Sciences. *Special Issue* on CHEMICAL BONDING
DOI 10.1007/s12039-016-1148-3

Role of Ti doping and Al and B vacancies in the dehydrogenation of $Al(BH_4)_3$

INDRANI CHOUDHURI, ARUP MAHATA, KUBER SINGH RAWAT and BISWARUP PATHAK*
Discipline of Chemistry and Discipline of Metallurgy Engineering and Material Science, Indian Institute of Technology (IIT) Indore, Indore, Madhya Pradesh 453 552, India
e-mail: biswarup@iiti.ac.in

MS received 5 April 2016; revised 28 June 2016; accepted 6 July 2016

Abstract. Metal borohydrides such as $Al(BH_4)_3$ is thermodynamically very stable but has weak dehydrogenation property. In contrast, $Ti(BH_4)_3$ has less stability (25°C) but excellent dehydrogenation property. Hence, we have studied Ti-doped aluminium borohydride systems in order to improve the dehydrogenation property. Our density functional studies (DOS and pDOS) show that Ti interacts more strongly with the BH_4 unit and such strong interaction weakens the B-H bond and improves the dehydrogenation property. Ti-doped $Al(BH_4)_3$ system improves the overall stability due to the formation of a stronger Ti-B bond. Our study on defects in $Al(BH_4)_3$ suggests that B-defect system has the best dehydrogenation property compared to the pure and Ti-doped $Al(BH_4)_3$ systems.

Keywords. Borohydrides; doping; defects; dehydrogenation; hydrogen storage.

1. Introduction

The ever increasing demand for energy and the serious problems with the fossil fuel burning lead us to search for various sources of alternative energies. The search for clean alternative fuel is the subject of recent interest. Hydrogen is one such promising alternative[1–3] as hydrogen has twofold more specific energy than its closest competitor methane.[4] Therefore, H_2 has the potential to sustain the growing demand of energy.[4] The United States department of energy (DOE) has set the target of 5.5% gravimetric capacity by 2020.[5] Such target pushed the search for materials with high hydrogen gravimetric density and better dehydrogenation property. The energetics for dehydrogenation pathways is one of the important thermodynamical criteria for the hydrogen-based fuels.

Metal borohydrides such as $LiBH_4$, $NaBH_4$, $Mg(BH_4)_2$, $Be(BH_4)_2$, $Zn(BH_4)_2$, $Cu(BH_4)_2$, $Al(BH_4)_3$, $Ti(BH_4)_3$, $Mn(BH_4)_2$, and $Y(BH_4)_3$[6–13] are very promising materials for hydrogen storage. Among all the metal borohydrides, $Al(BH_4)_3$ has the second highest hydrogen density (16.9%) after $LiBH_4$ (18.5%). Interestingly, the hydrogen desorption in $Al(BH_4)_3$ starts at 150°C[14,15] which is better than in $LiBH_4$ (470°C), $NaBH_4$ (595°C) and $Mg(BH_4)_2$ (323°C). On the other hand, borohydrides such as $Ti(BH_4)_3$ (25°C), $Mn(BH_4)_2$ (177°C), $Zn(BH_4)_3$ (85°C), $Sc(BH_4)_3$ (260°C), and $Zr(BH_4)_3$ (250°C)[16,17] were reported to be highly unstable and have lower desorption temperature and thus not suitable for practical usages. $Al(BH_4)_3$, is a well-known material for rocket-fuel with higher desorption temperature and better thermodynamic stability whereas similar borohydride such as $Ti(BH_4)_3$ is thermodynamically unstable at room temperature. $Al(BH_4)_3$ was first synthesized[18] in 1955 by treating $Al_2(CH_3)_6$ with B_2H_6 but the best way to synthesize is through the mechanochemical exchange reaction between $AlCl_3$ and $NaBH_4$. It is a liquid at the ambient condition with the boiling point of 36°C. Low-temperature single crystal X-ray diffraction[18] and DFT study[15] show that α-phase with C2/c space group is the more stable phase than the β-phase with $Pna2_1$ space group. The full dehydrogenation of $Al(BH_4)_3$ occurs *via* two steps (steps 1 and 2) and the dehydrogenation starts around 150°C.

$$Al(BH_4)_3 \rightarrow AlH_3 + 3B(s) + 9/2H_2 \quad (1)$$

$$AlH_3 \rightarrow Al(s) + 3/2H_2 \quad (2)$$

On the other hand, $Ti(BH_4)_3$ can be synthesized using $LiBH_4$ reacting with $TiCl_3$ or $TiCl_4$.[19] It is a volatile solid and XRD pattern confirms that the molecular structure of $Ti(BH_4)_3$ is similar to the $Al(BH_4)_3$ structure.[20] The $Ti(BH_4)_3.5NH_3$ structure has a space group of P222 or $P222_1$ and each Ti is surrounded by three (-BH_4) groups.[21]

*For correspondence
Celebrating 100 years of Lewis Chemical Bond

The dehydrogenation mechanism[6] (steps 3 and 4) of $Ti(BH_4)_3$ is as follows where the dehydrogenation starts at 25°C.

$$Ti(BH_4)_3 \rightarrow TiH_2 + 3B(s) + 5H_2 \quad (3)$$

$$TiH_2 \rightarrow Ti(s) + H_2 \quad (4)$$

Therefore, metal borohydrides such as $Al(BH_4)_3$ is thermodynamically stable but have weak dehydrogenation property. On the other hand, $Ti(BH_4)_3$ has excellent dehydrogenation property but less thermodynamic stability (25°C). So, we have considered Ti-doping in $Al(BH_4)_3$ to improve its dehydrogenation property and thermodynamic stability.

Numerous studies have been done to improve the dehydrogenation property of the metal borohydrides[22–27] and very recently Liu *et al*.,[27] showed that the dehydrogenation energy can be reduced significantly by making bimetallic borohydrides.

Ti is reported to be a very good doping material for improving the dehydrogenation property of the metal hydrides and borohydrides.[6,28–35] Recently Shi *et al.*,[30] reported that Ti-doping significantly improves the dehydrogenation property of the $Mg(BH_4)_2$ system. Ti prefers to occupy the Mg-site rather than B-site.[30] If Ti occupies the Mg and B sites of the $Mg(BH_4)_2$ then the atomic dehydrogenation energy decreases by 0.01 eV and 0.21 eV, respectively. Such doping leads to the formation of a bimetallic system, which in turn improves its dehydrogenation property. Due to the size mismatch of B and Ti, the Ti occupation energy is quite high at the B-site (2.41 eV) but favourable at the Mg-site.[30] Therefore in this work, we have considered Ti-doping in the Al-site in $Al(BH_4)_3$ to improve its dehydrogenation property.

Therefore, the low dehydrogenation temperature of $Ti(BH_4)_3$ (25°C) and good Ti occupation energy motivated us to study Ti doping in $Al(BH_4)_3$ system. We have performed the first principles calculation to investigate the Ti doping effect on the pure aluminium borohydride. The thermodynamic stability and hydrogen desorption property of the Ti-doped $Al(BH_4)_3$ system is thoroughly studied and compared with the pure $Al(BH_4)_3$ system.

Like doping, defects also play an important role to improve the dehydrogenation property[36] of the metal hydride systems. Therefore, keeping all these in mind, we have studied the Al and B defects in pure $Al(BH_4)_3$ and Ti-doped $Al(BH_4)_3$ systems for improving their dehydrogenation property. Previous reports[37,38] suggest that the dehydrogenation energetics is varied with temperature and H_2 partial pressure for $NaBH_4$ and MgH_2 systems. Here, we have done the comparative study to show the role of Ti doping and Al/B defects in the dehydrogenation property of $Al(BH_4)_3$.

2. Computational Methods

First principle calculations within the framework of density functional theory were performed using Vienna *Ab initio* simulation package (VASP).[39] The exchange-correlation potential was described by using the generalized gradient approximation of Perdew-Burke-Ernzerhof (GGA-PBE).[40] Projector augmented wave (PAW) method[41] was employed to treat interactions between ion cores and valance electrons. Plane wave with a kinetic energy cut off of 385 eV was used to expand the electronic wave functions. We have included the semi-empirical DFT-D3 dispersion energy correction (Grimme's D3 corrections)[42] for the dehydrogenation energy calculations to get the most accurate results. The Brillouin zone of the aluminium borohydride unit cell (a=18.20 Å, b=6.13 Å, and c=6.19 Å; 64 atoms) was sampled with a $1\times3\times3$ Monkhorst-pack k-point grid.[43] We have constructed a supercell (a=18.20 Å, b=18.20 Å, and c=18.20 Å) of 576 atoms to study the doped and defect-systems. The Brillouin zone of the supercell was integrated with a $1\times1\times1$ (Γ points) Monkhorst-pack k-point grid. Structures were fully relaxed where the total energy and Hellmann−Feynman forces are set at 10^{-4} eV and 10^{-3} eV/Å, respectively. The density of states (DOS) of the pure $Al(BH_4)_3$ was calculated using the optimized structure of the unit cell with a Monkhorst-pack generated sets of $3\times9\times9$ k-points. DOS calculations of the doped and defect-systems were done on the supercell structure with Monkhorst-pack generated sets of $3\times3\times3$ k-points.

3. Results and Discussion

We begin the analysis by studying the hydrogen storage and electronic properties of the pure $Al(BH_4)_3$ system. A relationship is then brought between the pure and Ti-doped $Al(BH_4)_3$ systems to understand the effect of Ti doping on the stability, hydrogen storage and electronic properties of the pure system. The role of the Al and B defects in the dehydrogenation property of the $Al(BH_4)_3$ and Ti-doped-$Al(BH_4)_3$ systems is discussed at the end.

3.1 *Pure aluminium borohydride*

The orthorhombic β-$Al(BH_4)_3$ structure (space group $Pna2_1$) is studied for the hydrogen storage property. The CIF (Crystallographic Information File) data[18] of

the β-$Al(BH_4)_3$ is taken from the Cambridge Crystallographic Data Centre (CCDC, reference no. 186/404). The optimized structure of the $Al(BH_4)_3$ is shown in Figure 1(a). The optimized crystal parameters and Wyckoff positions are calculated and summarized in Table S1 (Supporting Information). We find our calculated bond lengths (Al-B = 2.13 Å; B-H = 1.23 Å) are very much comparable with the previous theoretical[15] (Al-B = 2.15 Å; B-H = 1.21 Å) and experimental data (Al-B: 2.12 Å and B-H: 1.20 Å).[18]

The total electron density of the pure aluminium borohydride system is presented in Figure 1(b) and it shows that electron density is mainly localized on the ($-BH_4$) units of the aluminium borohydride structure. The less electron density overlap between the Al and BH_4 group implies strong ionic interactions between the Al and BH_4 groups.

The molecular $Al(BH_4)_3$ structure is presented in Figure 1(c). In the $Al(BH_4)_3$ unit, each BH_4 has two types of hydrogen, H1 and H2 hydrogen atoms which are in close proximity, and H3 and H4 which are far from the Al centre. We have calculated atomic hydrogen removal energy for the terminal ($H_{Terminal}$) and bridge (H_{Bridge}) hydrogen atoms. Similarly, molecular H_2 removal energy (E_{H2}) is calculated for four different pairs of hydrogen (Figure 1(c)) to understand its dehydrogenation property. The first pair (H_A) of the hydrogen (H1 and H2) is the equivalent hydrogen of the same BH_4 unit. The second pair (H_B) of hydrogen is the non-equivalent hydrogen (H2 and H3) of the same BH_4 unit. The third pair (H_C) of the hydrogen is the terminal hydrogen (H3 and H4) and fourth pair (H_D) of the hydrogen (H2 and H6) is from two different BH_4 units. The atomic and molecular[44–46] hydrogen removal energies are calculated using the equations 5 and 6 respectively.

$$E_H = (E(Al_{36}B_{108}H_{431}) + 1/2E_{[H2]}) - E(Al_{36}B_{108}H_{432}) \quad (5)$$

$$E_{H2} = (E(Al_{36}B_{108}H_{43}) + E_{[H2]}) - E(Al_{36}B_{108}H_{432}) \quad (6)$$

Here E_H and E_{H2} represent atomic and molecular dehydrogenation energies, respectively. The energies of the structures are taken from their fully relaxed geometries whereas single point energy is calculated for the $Al_{36}B_{108}H_{430}$ structure within the geometry of $Al_{36}B_{108}H_{432}$. A similar convention is used to calculate the atomic dehydrogenation energy. The hydrogen atomic and molecular energies (E_{H2}) are calculated by putting H and H_2 into a cubic box of 10 Å sides.[30] Our calculated H-H bond length (0.74 Å) is very much in agreement with the previously calculated value of 0.74 Å.[38]

We have calculated atomic dehydrogenation energies (E_H) for the terminal and bridge hydrogens of

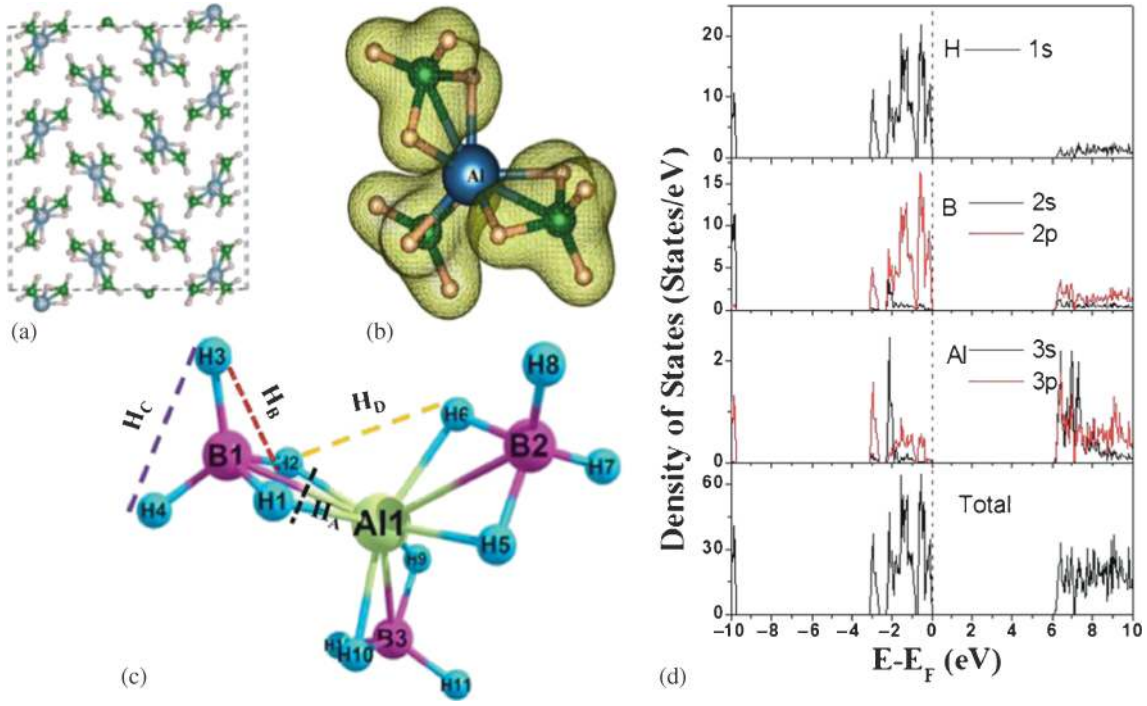

Figure 1. (a) The optimized supercell structure of $Al(BH_4)_3$ (a = 18.20 Å, b = 18.41 Å and c = 18.59 Å). (b) Electron density around the $Al(BH_4)_3$ unit (Isosurface value: 0.039 e.Å^{-3}). (c) Molecular structure of $Al(BH_4)_3$ with four pairs (H_A, H_B, H_C and H_D) of hydrogen atoms. (d) Total and partial density of states of pure aluminium borohydride. The Fermi level is set to zero and indicated by a black-dashed line.

pure $Al(BH_4)_3$ and presented in Table 1. We find that the bridge hydrogen has lower dehydrogenation energy (2.31 eV) than the terminal hydrogen (3.37 eV). This is because of the longer B-H bond distance (1.26 Å) in bridge hydrogen than in the terminal one ($B\text{-}H_{Terminal}$=1.20 Å). The calculated molecular dehydrogenation energies (Table 1) for H_A, H_B, H_C and H_D pairs are 4.18, 4.36, 4.46 and 3.72 eV, respectively. Therefore, the hydrogen removal energy follows the $H_C > H_B > H_A > H_D$ order. The dispersion energy calculated using Grimme's D3 corrected energies (Table 1) are very much in agreement with the calculated values using GGA–PBE level of theory. Therefore, we have not discussed these values. But for comparison, these values are tabulated in Table 1.

The highest and lowest H_2 removal energy is found for H_C and H_D pair of hydrogen respectively. The Bader charge analysis (Table S2, Supporting Information) is done using Atoms in Molecules (AIM) theory[47–50] to understand the hydrogen removal trend. The Bader charges on the H_A pair of hydrogen atoms are 1.65e (−0.65) and 1.62e (−0.62). For the H_B (H2 and H3) pair, the charges on the hydrogen atoms are 1.62e (−0.62) and 1.49e (−0.49) respectively. In the case of H_C pair (H3 and H4), hydrogen possesses similar charges (1.49e) due to the similar nature of the hydrogen. In the case of H_D pair (H2 and H6), the charges on the hydrogen atoms are 1.62e (−0.62) and 1.63e (−0.63), respectively. So the charges on the hydrogen atoms are similar for all hydrogen atoms except for H_B pair (H2 and H3) (Table S2, Supporting Information). But the hydrogen removal energy is different for different pairs.

H_C pair requires higher hydrogen removal energy compared to H_B pair. This could be explained from the B-H bond lengths. H_A (B1-H1 and B1-H2) pair consists of bridge hydrogen which is longer (1.26 Å) compared to H_D pair (B1-H2 and B2-H6) where one of the hydrogens is a terminal one (B-H = 1.20 Å). On the other hand, in the H_B and H_C pairs, at least one hydrogen atom is a terminal hydrogen (1.20 Å), thus requiring higher hydrogen removal energy compared to H_A/H_D pair.

The total and partial density of states (TDOS and pDOS) of pure Al-borohydride system are presented in Figure 1(d). The calculated band gap (6.18 eV) of the pure system is very much comparable with the previous study (6.20 eV)[15] pDOS study shows (Figure 1d) H *1s* orbital densities are concentrated in two separate regions. B *2p* orbitals are located in the −0.75 eV to 0 eV energy region. On the other hand B *2s*/*2p* orbital's amplitudes are lower and located in the lower energy region (−2.25 eV to −0.75 eV). H *1s* orbital is also located in the same energy region (−2.25 eV to −0.75 eV). This implies that covalent B-H bonding is present in the $Al(BH_4)_3$ system. The partial density of states (pDOS) show that the H *1s* Al *3s* and Al *3p* orbitals are present in the −3.0 eV to 0 eV energy region which implies Al-H *sp* mixing in the Al-borohydride system. The bridge-bonded hydrogen atoms are energetically in the higher position than the terminal B-H bonds (Figure S2 in SI). So these bridge hydrogen atoms are easy to dehydrogenate than the terminal one. This is also reflected in their molecular dehydrogenation energies where H_D and H_C pairs require lower (3.72 eV) and higher (4.46 eV) hydrogen removal energy respectively.

3.2 *Ti-Doped-Al(BH₄)₃*

The Ti doping on the $Al(BH_4)_3$ system is studied by doping 1 to 4 Ti atoms in the Al-site of the supercell (Al=36, B=108, H=432), thus the doping concentrations

Table 1. The calculated atomic (E_H) and molecular (E_{H2}) dehydrogenation energy of the pure and Ti-doped $Al(BH_4)_3$ systems. The values with asterisk (*) denote the dispersion corrected dehydrogenation energies.

Compounds	Ti-Doping Concentration (%)	Atomic Dehydrogenation Energy (eV)		Molecular Dehydrogenation Energy (eV)			
		$H_{Terminal}$	H_{Bridge}	H_A	H_B	H_C	H_D
$Al(BH_4)_3$	0.00	3.37	2.31	4.18	4.36	4.46	3.72
		3.43*	2.36*	4.27*	4.41*	4.56*	3.81*
$Ti_xAl_{1-x}(BH_4)_3$	2.78	2.20	1.29	2.74	3.71	3.71	3.17
		2.29*	1.36*	2.83*	3.83*	3.83*	3.83*
$Ti_xAl_{1-x}(BH_4)_3$	5.56	2.11	1.10	3.07	4.02	4.02	3.41
		2.19*	1.15*	3.16*	4.13*	4.13*	3.52*
$Ti_xAl_{1-x}(BH_4)_3$	8.33	2.08	1.09	3.02	3.98	3.98	3.43
		2.16*	1.17*	3.12*	4.09*	4.09*	3.53*
$Ti_xAl_{1-x}(BH_4)_3$	11.11	2.07	1.08	3.02	3.87	3.98	3.41
		2.15*	1.16*	3.12*	3.99*	4.09*	3.56*

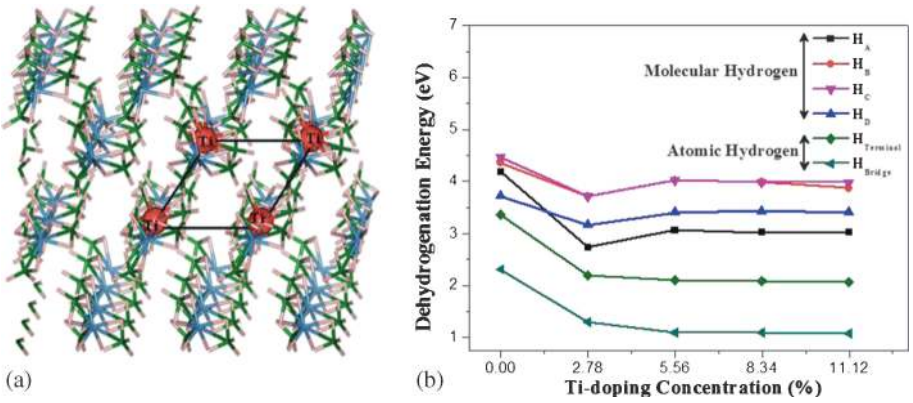

Figure 2. (a) The rectangular Ti_4 doping pattern in $Al(BH_4)_3$ supercell. (b) Change in molecular dehydrogenation energy (eV) with increasing Ti-doping concentration.

range from 2.78% (Ti=1), 5.56% (Ti=2), 8.33% (Ti=3) to 11.11% (Ti=4) (Figure 2(a)). The lowest and highest doping concentrations are 2.78% and 11.11%, respectively. Ti doping is done in such a way that the distances between the Ti-atoms are minimum (Figure 2(a)).

The dopant's (Ti) occupation energy is calculated using the following equation.

$$E_O = E(Al_{36-x}Ti_xB_{108}H_{432}) - E(Al_{36}B_{108}H_{432}) - x[E(Ti_{hcp}) - E(Al_{fcc})] \quad (7)$$

Here, E_O represents the occupation energy of the Ti dopant for various doping concentrations [2.78% (x=1), 5.56%(x=2), 8.33% (x=3), and 11.11%(x=4)]. Their respective energies are calculated from the Ti doped systems, pure $Al(BH_4)_3$ system, hexagonal close packed (hcp) Ti and face centred cubic (fcc) Al bulk structures, respectively. The relaxed Ti-doped structure shows that Ti is surrounded by three (-BH_4) units as in pure $Al(BH_4)_3$ structure. The calculated occupation energies are −4.54 eV, −8.84 eV, −12.88 eV and −16.91 eV for 2.78%, 5.56%, 8.33%, and 11.11% Ti doping concentrations, respectively. The negative occupation energies (E_o) indicate that the Ti doping is thermodynamically favourable. But when we compute the occupation energy per Ti-atom the calculated occupation energies are −4.54 eV (2.78%), −4.42 eV (5.56%), −4.29 eV (8.33%), and −4.23 eV (11.11%) respectively. It indicates that the overall stability of the doped systems reduces with increase of Ti. Recently, Shi *et al.*,[30] also reported that Ti doping is favourable at the Mg site than B site in the $Mg(BH_4)_2$ system. We have also calculated Ti occupation at the B site of $Al(BH_4)_3$ system and we find that Ti doping is not favourable at the B-site (E_O = 2.21 eV) of $Al(BH_4)_3$. Therefore, we did not consider such a system [Ti doping at the B-site of $Al(BH_4)_3$] for improving dehydrogenation property.

To understand the Ti doping in Al-borohydride system, we have investigated the Ti-substitution in the molecular level (Figure 3a). To do this, we have optimized $Al(BH_4)_3$ and Ti substituted $Al(BH_4)_3$ [i.e., $Ti(BH_4)_3$] molecules. The reaction energy for the

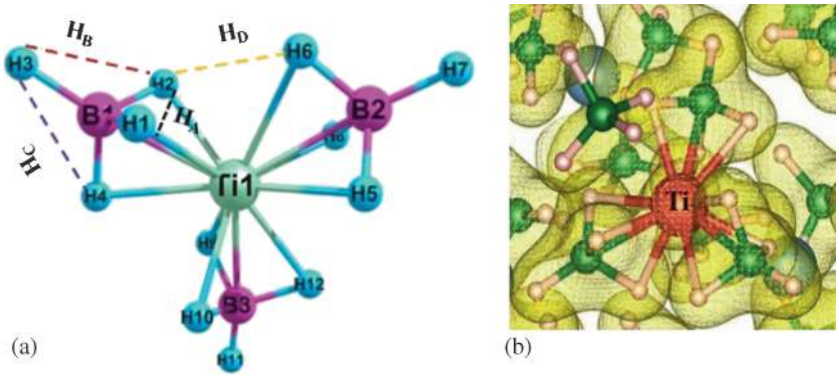

Figure 3. (a) Ti-doped aluminium borohydride molecular unit. (b) Projection of total electron density of 2.78% Ti-doped $Al(BH_4)_3$ (Isosurface value: 0.039 e.Å^{-3}).

formation of $Ti(BH_4)_3$ molecule is calculated using the following equation:

$$E_F = [E_{Ti(BH4)3} - E_{Al(BH4)3}] - [E(Ti_{hcp}) - E(Al_{ccp})] \quad (8)$$

where, $E_{Ti(BH4)3}$ and $E_{Al(BH4)3}$ are the energies of the titanium and aluminium borohydride molecules, respectively. The calculated reaction energy (−3.27 eV) shows $Ti(BH_4)_3$ formation is highly favourable at the molecular level.

Therefore, the Ti negative occupation energy indicates the $Ti(BH_4)_3$ unit is stabilized due to the Ti-B and Ti-H bond formation. The vacant Ti 3*d* orbital interacts with the H atoms in close proximity (Figure 3a–b), thus forming a stable $Ti(BH_4)_3$ structure. For the 2.78% Ti-doped $Al(BH_4)_3$ system, three Ti-H bonds are formed. Hence, such doping changes the bonding pattern of the $Al(BH_4)_3$ unit. Such bond formation certainly stabilizes the molecular unit of the doped structure. Now, as the doping concentration increases from 5.56% to 11.11%, the number of Ti-H bond increases which favours the occupation.

Atomic and molecular hydrogen removal energies are calculated by removing H and H_2 from the $Ti(BH_4)_3$ unit of the supercell. The Ti-doping is done in such a way that Ti-Ti distances are minimum to introduce bi-, tri- and tetra-metallic systems. In the optimized Ti-doped structures, the Ti-Ti distances are more than 6.0 Å, which is much higher than the Ti-Ti distance (2.89 Å)[51] in a Ti-cluster, thus reducing the possibility of cluster formation.

More importantly, the Ti removal energy ($E_{Ti\text{-}removal}$) and cohesive energy ($E_{Cohesive}$) are calculated to rule out the possibility of cluster formation.

$$E_{Ti\text{-}removal} = E(TiAl_{35}B_{108}H_{432}) - [E(Al_{35}B_{108}H_{432}) + E(Ti)] \quad (9)$$

$$E_{Cohesive} = [E(Ti_{hcp}) - nE(Ti)]/n \quad (10)$$

Here, Ti energy, E(Ti) is calculated by putting Ti atom into a cubic box of 18 Å sides. The calculated Ti removal energy (16.33 eV) is much higher than the Ti-cohesive energy (6.17 eV); thus we have ruled out any possibility of aggregation which could lead to the formation of most stable (hcp) Ti-bulk structure. Therefore, such doping will have the maximum influence on the hydrogen desorption property as reported previously.[27]

The dehydrogenation energies of the Ti-doped systems are calculated (Table 1) using the following equations.

$$E_{H2} = (E(Al_{36-x}Ti_xB_{108}H_{430}) + E_{[H2]}) - E(Al_{36-x}Ti_xB_{108}H_{432}) \quad (11)$$

$$E_H = (E(Al_{36-x}Ti_xB_{108}H_{430}) + 1/2E_{[H2]}) - E(Al_{36-x}Ti_xB_{108}H_{432}) \quad (12)$$

Here also, hydrogen removal energy is studied for atomic hydrogen and the same pairs of hydrogen H_A (equivalent), H_B (non-equivalent hydrogen), H_C (terminal hydrogen) and H_D (from different BH_4 unit) as in the pure $Al(BH_4)_3$ system (Figure 3a).

In the Ti-doped systems, the atomic hydrogen removal energies are reduced significantly (Table 1) and the trend in dehydrogenation energies remains same for the terminal and bridge hydrogen atoms. Interestingly, the molecular hydrogen removal energy trend in the Ti-doped systems is a little different, $H_C \geq H_B > H_D > H_A$ from the pure system, $H_C > H_B > H_A > H_D$. Looking at the structural unit of the $Ti(BH_4)_3$ system (Figure 3b), we find there is a change in the orientation of the hydrogen atoms of the BH_4 unit. In the Ti-doped system, it shows nine hydrogen atoms are bridge bonded (between B and Ti) in comparison to six in the pure system.

In the Ti mono-doped system, with respect to the pure system, the distance between hydrogen decreases from 2.10 to 1.97 Å and 2.48 to 2.28 Å and increases from 1.96 to 2.06 Å for the H_A and H_D and H_B pair of hydrogens, respectively. Due to doping, the distance (Table S2, Supporting Information) between the H_D (2.28 Å) and H_A (1.97 Å) pair of hydrogens decreases but increases in H_B (2.06 Å) pair whereas it remains constant in H_C.

The molecular dehydrogenation energy is lowest (2.74 eV) for the H_A pair and highest (3.71 eV) for the H_B and H_C pairs. In the Ti-doped systems, each BH_4 unit has three bridge-bonded hydrogens and the H1-H2 distances (H_A pair 1.97 Å) are very close to the van der Waals radius (1.91 Å) of H_2 gas, thus easier to remove. In the case of H_D pair of hydrogens, both the hydrogen atoms are bridge-bonded compared to H_B and H_C pairs where one of the hydrogen atoms is a terminal one. As bridge hydrogen has longer B-H bond lengths compared to terminal hydrogen, it is easier to remove. Therefore, we find 2.78% Ti-doping could lower the hydrogen removal energies by 1.44 eV, 0.65 eV, 0.75 eV and 0.55 eV for the H_A, H_B, H_C, and H_D pair of hydrogens, respectively (Figure 2b).

But as we increase the Ti doping concentration, the atomic and molecular dehydrogenation energy increases but still lower than the pure aluminium borohydride system. This can be explained from the extra stability gained by the Ti-doped structures. When we dope a second Ti atom in the vicinity of the first Ti atom, we find Ti-Ti interactions are present in the system, which gives them an extra stability. This is reflected in their occupation energy too. But as we increase the Ti-doping concentration from 8.83% to 11.11%, the extent of Ti-Ti interactions is similar. So there are not much changes in the atomic and molecular hydrogen

removal energies. So, we concluded that the atomic and molecular hydrogen removal trends remain same in the Ti-doped $Al(BH_4)_3$ systems.

We have done the Bader charge analysis for the Ti doped systems and we find the hydrogen atoms are more positively charged than in the pure system. This may be due to the mixing of H 1*s* and Ti 3*d*-orbitals. Due to this, the charges on the H_A, H_D pair of hydrogen atoms are similar. In the case of H_A pair (H1 and H2) the Bader charges on the both hydrogen are same (1.48e) and for H_D pair (H2 and H6), the charges are 1.48e (−0.48) and 1.47e (−0.47) respectively. But in H_B (H2 and H3) and H_C (H3 and H4) pairs, they have different charges 1.48e (−0.48) and 1.53e (−0.53), (Table S2, Supporting Information) as they are different type of hydrogens. So, such charge differences explain the molecular dehydrogenation energy trend ($H_C \geq H_B > H_D > H_A$) in the 2.78% Ti-doped system. The more charge differences between the H- and B-atoms make them a polar bond. As shown in Table S2 (Supporting Information), the B-H bond length increases in the doped system. So, Ti doping certainly weakens the B-H bond which in turn decreases the molecular dehydrogenation energy. Now, as we increase the Ti doping concentration (to 5.56%), the molecular dehydrogenation energy increases but not significantly. The total electron density of the 2.78% Ti-doped aluminium borohydride system (Figure S1(a), Supporting Information) clearly shows electron density overlap between the Ti and the hydrogen of the BH_4 unit. Therefore, covalent interaction is present between the Ti and BH_4 group.

In Figure 4a, we have plotted the TDOS and pDOS of 2.78% Ti-doped Al-borohydride system. The Ti *3d* orbital density is mainly localized in the lower (−5.5 eV to −4.0 eV) energy region. There are some orbital overlaps between the Ti, B and H orbitals which support the formation of $Ti(BH_4)_3$ structure with the super cell of $Al(BH_4)_3$. The stabilization of the valence band of the doped and defect-system is done with respect to the B *2s* orbital, which is far from the doping/defect-site. Due to the Ti-doping, the valence band edge is stabilized by 3.50 eV with respect to the pure system. So, the valence band edge is shifted in the lower energy region (Figure 4a). To our surprise, the valence band edge (Figure 4b) is further stabilized (by 0.10 eV) when we increase the doping concentration to 5.56%. Therefore, Ti-doping certainly stabilizes the whole system.

Shi *et al.* reported Ti doping at the Mg site of $Mg(BH_4)_2$ is thermodynamically favourable but such a doping did not improve its dehydrogenation property significantly.[23] However, we report, here that Ti doping at the Al site of the $Al(BH_4)_3$ is thermodynamically very much favourable and such doping improves its dehydrogenation property significantly.

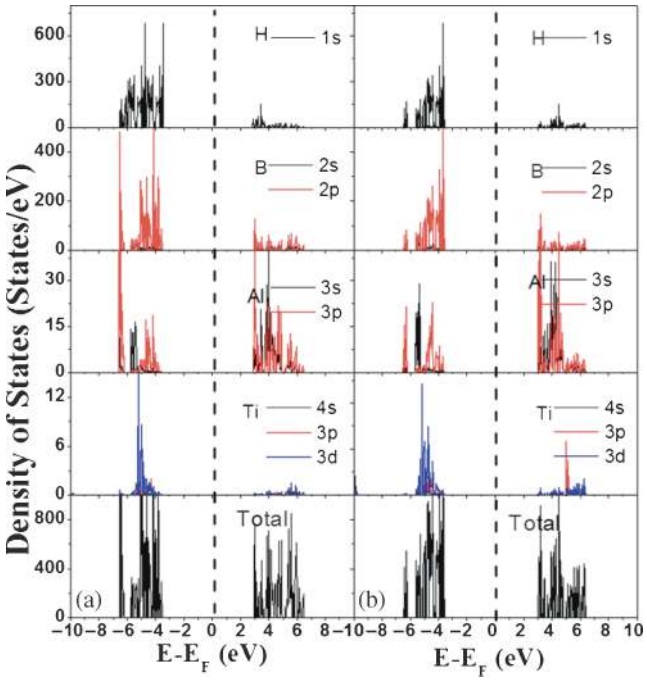

Figure 4. Total and partial density of states of (a) 2.78% and (b) 5.56% Ti-doped $Al(BH_4)_3$ systems. The Fermi level is set to zero and indicated by a black-dashed line.

3.3 *Al/B Defect Study in Pure and Ti-doped systems*

It has been reported that defects could play a vital role in the dehydrogenation property of the hydrogen storage materials.[36] Thus, if we create Al defects in the $Al(BH_4)_3$ system, the dehydrogenation property of the $Al(BH_4)_3$ system can be improved. Similarly, B-defects in $Al(BH_4)_3$ system will improve its dehydrogenation property.[52] Thus, we have studied the role of Al and B vacancies in pure and doped $Al(BH_4)_3$ system to improve their dehydrogenation property.

We have created Al and B-defects in the $Al(BH_4)_3$ system of deleting Al and B atoms which lead to the defect concentrations of 2.78% and 0.93%, respectively. The Al/B defect formation energy is calculated using the following equations.

$$E_{f(Al)} = [E(Al_{35}B_{108}H_{432}) + E_{(Al-ccp)}] - E(Al_{36}B_{108}H_{432}) \quad (13)$$

$$E_{f(B)} = [E(Al_{36}B_{107}H_{432}) + E_{(B\text{-}rhombohedral)}] - E(Al_{36}B_{108}H_{432}) \quad (14)$$

The calculated defect formation energies are 3.49 eV and 2.24 eV for Al and B defects in $Al(BH_4)_3$ system, respectively. Therefore, Ti doping is thermodynamically

Table 2. Atomic (E_H) and Molecular (E_{H2}) dehydrogenation energies of the Al/B-defects in pure and Ti-doped $Al(BH_4)_3$ systems. The values with asterisk (*) denote the dispersion corrected dehydrogenation energies. The values in the parenthesis are H-H bond distances in Å.

Compound	Defect Formation Energy (eV)		Atomic Dehydrogenation Energy (eV)	Molecular Dehydrogenation Energy(eV) H_A	H_B	H_C	H_D
Al-defect	Pure	3.49	2.42	1.60	1.92	1.89	1.49
				1.68*	2.01*	1.97*	1.58*
				(1.94)	(2.26)	(2.20)	(2.19)
	Doped	1.84	2.13	1.80	1.07	1.53	3.20
				1.91*	1.16*	1.64*	3.32*
				(2.21)	(0.84)	(1.78)	(2.24)
B-defect	Pure	2.24	1.96	0.50	1.19	0.004	0.29
				0.61*	1.26*	0.009*	0.37*
				(1.62)	(2.51)	(0.75)	(2.49)
	Doped	1.67	0.44	1.83	2.99	0.03	1.89
				1.91*	3.09*	0.05*	1.97*
				(1.94)	(2.19)	(0.76)	(2.57)

favourable over Al (2.78%) and B-defect (0.93%) in pure $Al(BH_4)_3$ system.

We have also studied the Al and B defects in the Ti-doped (2.78%) aluminium borohydride system. We have calculated the formation energies of the Ti-doped Al/B defect-systems using the following equations.

$$E_{f(Ti-Al)} = [E(Al_{34}TiB_{108}H_{432}) + E_{(Al-ccp)}] - E(Al_{35}TiB_{108}H_{432}) \quad (15)$$

$$E_{f(Ti-B)} = [E(Al_{35}TiB_{107}H_{432}) + E_{(B-rhombohedral)}] - E(Al_{35}TiB_{108}H_{432}) \quad (16)$$

Here, $E_{f(Ti-Al)}$ and $E_{f(Ti-B)}$ are the formation energies of the Ti-doped-Al-defect system and Ti-doped-B-defect system, respectively. The calculated formation energies (Table 2) are 1.84 and 1.67 eV for Ti-doped-Al-defect system and Ti-doped-B-defect system, respectively. Therefore, such doped-defect systems are more stable than their respective defect systems.

3.4 *Al defect in Pure and Ti-doped (2.78%) aluminium borohydride system*

We have modelled Al-defect in pure $Al(BH_4)_3$ system (Figure 5a) by removing one Al atom from the $Al(BH_4)_3$ supercell. For the Ti-doped system, we have deleted the Al atom closest to the $Ti(BH_4)_3$ unit. There are many studies where they have reported that doping favours defect formation.[53,54] Zhang *et al.*,[53] using first principle study reported that Mg and Al doping influences the Frenkel defect in the $LiBH_4.NH_3$ structure due to thermal instability of the structure. So, when Al defect is created in the vicinity of the Ti-doped unit, then the $Ti(BH_4)_3$ unit is slightly distorted due to the formation of Ti-B bonds. A structural deformation is noticed in the tetrahedral $Ti(BH_4)_3$ unit (Figure 5b).

The total charge density of the Al-defect system and Ti-doped Al-defect system is presented in Figure S1(b-c) (Supporting Information). The dehydrogenation energy of the Al-defect system is calculated for the four pairs (Figure 5a) of hydrogen (H_A, H_B, H_C, and H_D) as in the pure and Ti-doped systems. After Al removal, H_A, H_B and H_C pairs of hydrogen belong to same BH_4 unit but H_D from two different BH_4 units. From our calculations, we find that Al vacancy destabilizes the system (Figure 5a) which facilitates the hydrogen evolution process.[38] The dehydrogenation energy sequence becomes H_B(1.92 eV)>H_C (1.89 eV)> H_A(1.60 eV)>H_D (1.49 eV). So, the dehydrogenation energy of the Al-borohydride system decreases due to the defect (Al) in the system. H_B has the highest molecular dehydrogenation energy because the two hydrogen atoms are strongly bonded to B atom (B-H =1.22-1.23 Å). H_C pair has similar molecular dehydrogenation energy because of the same nature of the H. Actually, H_A pair has longer B-H bonds (1.28 Å) compared to H_B and H_C pairs (1.20 Å). Thus, H_A pair has lower dehydrogenation energy than the H_B and H_C pairs H_D has the lowest molecular dehydrogenation energy because one of the B-H is elongated one (1.34 Å), which is longer than the normal B-H distance. So, the B-H bond dissociation is much easier than in the pure system, hence justifying the order (H_B >H_C >H_A >H_D) of the molecular dehydrogenation energy. The hydrogen removal energy is calculated for another pair (H_E, Figure 5a) of hydrogen because of the short hydrogen-hydrogen distance (0.86 Å). So, the molecular dehydrogenation energy of this pair (H_E) is lowest (1.10 eV).

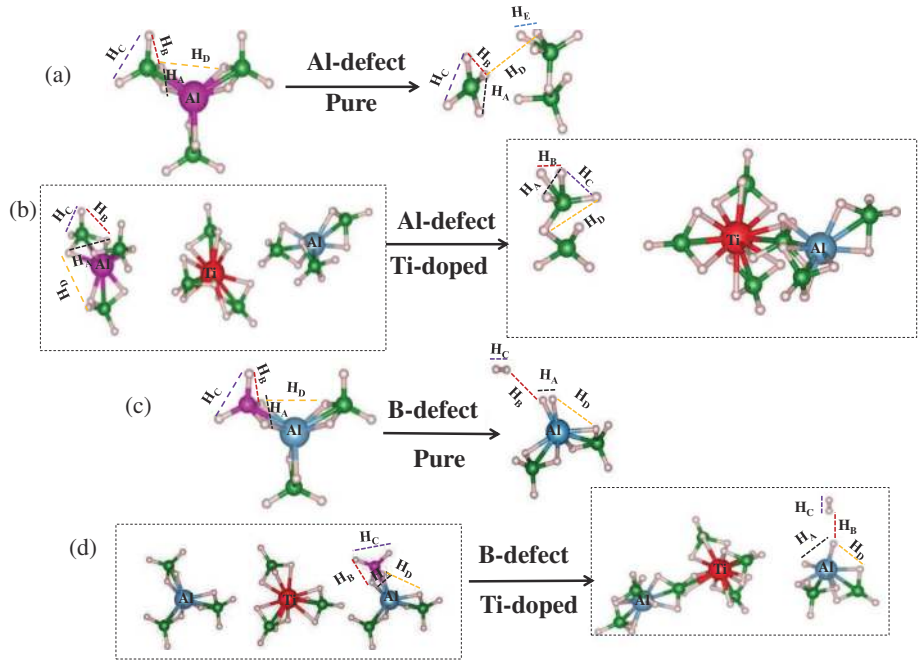

Figure 5. Schematic representation of (a) Al-defect system, (b) Ti-doped-Al-defect system, (c) B-defectsystem and (d) Ti-doped-B-defect systems.

The Al-defect in the 2.78% Ti-doped Al-borohydride system is studied by creating a vacancy in the vicinity of doped Ti atom. The dehydrogenation energy is calculated for the same pair of hydrogen (H_A, H_B, H_C, and H_D). Here, H_D needs higher removal energy (3.20 eV) than in the Al-defect system. This can be explained by the H-H distance (2.24 Å), which is longer than in the Al-defect system (2.19 Å). H_A pair of hydrogen needs little higher removal energy due to the stability of the Ti-doped-Al-defect system. The B-H bond distances in H_A pair are 1.20 Å and 1.19 Å. The B-H bond length of H_A pair is shortened in comparison to the Al-defect system. So the shorter B-H bond distance increases the molecular dehydrogenation energy. In the H_C pair, the H-H distance decreases (1.78 Å from 2.20 Å) in the doped-defect system and one of the B-H bond length increases to 1.34 Å. So the elongated B-H distance and shorter H-H distance decreases the molecular dehydrogenation energy. The dehydrogenation energy of the H_B (0.84 Å) set is the lowest (1.07 eV).

The dehydrogenation trend can be explained by the Bader charge analysis too. For the H_B pair, the B-H bonds are more polar (B-H charge difference: 1.51e) in the doped-defect system than in the Al-defect system (B-H charge difference: 1.44e). So in the doped-defect system, the molecular dehydrogenation energy for the H_B pair is lower in comparison to the Al-defect system. In H_D case, the charge difference between hydrogen is higher in Ti-dopedAl-defect (0.46e) than in pure Al-defect system (0.11e). In the Ti-doped-Al-defect $Al(BH_4)_3$ system, there are many non-equivalent hydrogen atoms, thus acquiring a different amount of positive charge. The differences in the positive charges are different from pair to pair, which in turn affects their removal. As H_2 is a non-polar molecule so the charge on H is almost same. As the charge difference between two H atoms decreases then they are easy to be removed. But the distance between the hydrogen in Ti doped-Al-defect system increases, so the H_D value.

In H_C pair, the B-H bonds are less polar in Al-defect system than in doped-defect system, thus H_C has lower molecular dehydrogenation energy in doped-defect system than in the Al-defect system. In Al-defect system the charge difference between H_A pair of hydrogen are zero but in the doped-defect system the H-H charge difference becomes 0.41e (in H_A pair of hydrogens). So the Bader charges justify the molecular dehydrogenation energy trends [H_D (3.20 eV) > H_A (1.80 eV) > H_C (1.53 eV) > H_B (1.07 eV)] in the Ti-doped Al-defect system.

3.5 *B-defect in pure and Ti-doped (2.78%) Al-borohydride systems*

Here, we have studied the B-defects in pure and 2.78% Ti-doped aluminium borohydride systems to improve their dehydrogenation property. In both the cases, B-defect concentration is 0.93%. We have modelled B-defect by deleting one B atom from the $Al(BH_4)_3$ unit cell and in case of Ti-doped system, the B atom

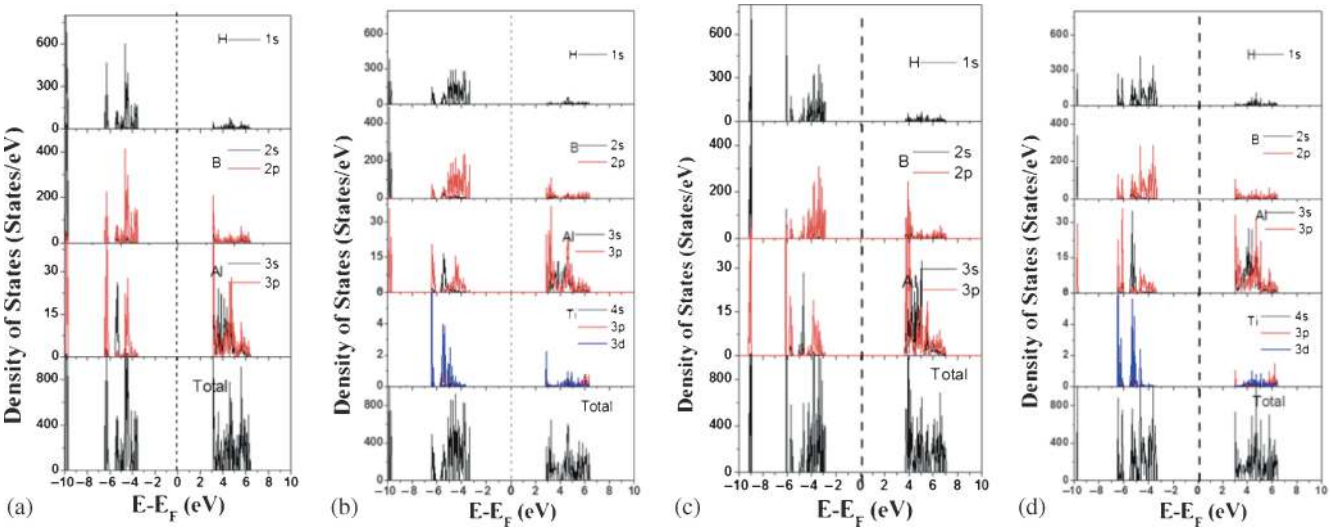

Figure 6. Total and partial density of states of (a) Al-defect system, (b) Ti-doped-Al-defect system, (c) B-defect system and (d) Ti-doped-B-defect system. The Fermi level is set to zero and indicated by a black-dashed line.

is deleted from the neighbouring $Al(BH_4)_3$ unit of the $Ti(BH_4)_3$ unit. This was done to have the maximum effect on their stability and dehydrogenation property. The B-defect formation is more favourable in the Ti-doped system (1.67 eV) than in the pure system (2.24 eV).

The hydrogen (H_A, H_B, H_C and H_D) removal energies are calculated for the B-defect system and Ti-doped B-defect system. These hydrogen pairs are shown in Figure S3a-b (Supplementary Information) for the B-defect system and Ti-doped-B-defect system. Due to the B-defect, one pair (H_C) of hydrogen will be evolved easily (Figure S3a–b in SI). Now in the B-defect system, the trends in molecular dehydrogenation energy is H_B (1.19 eV)>H_A (0.50 eV)>H_D (0.29 eV)>H_C (0.004 eV).

In comparison to the pure system, the molecular dehydrogenation energy of the B-defect system is lower for all hydrogen pairs. We find H_B pair of hydrogen needs higher removal energy than H_A, H_D, and H_C. This is because in the H_B pair, one of the hydrogen comes from the trapped H_2 molecule, which is difficult to dehydrogenate. $H_D > H_C$ can be explained by their bonding nature. In H_D one of the hydrogen atoms is bridge-bonded between Al and B and therefore difficult to remove. On the other hand for the H_C, the hydrogens are trapped as H_2 (Hydrogen atoms are 0.75 Å apart) and thus easy to remove. For the H_A pair, both the hydrogen atoms are directly bonded to Al, and thus has elongated Al-H bonds (1.69 Å).

The Al-H distance is also decreased in the Ti-doped B-defect system (1.61 Å) more than in the B-defect system (1.69 Å). This is the reason for higher hydrogen removal energy in the doped-defect system (1.83 eV) than in the defect system (0.50 eV). Here also H_B set needs higher hydrogen removal energy because one hydrogen is from the trapped H_2 molecule.

The TDOS and pDOS of Al-defect system and Ti-doped-Al-defect system are plotted in Figure 6a-b. In the case of Al-defect system, the valence band edge position is shifted in the lower energy region by 3.50 eV. On the other hand, these orbitals are destabilized by 0.14 eV in the Ti-doped-Al-defect system (Valence band edge is at −3.36 eV) in comparison to the 2.78% Ti-doped $Al(BH_4)_3$ system. The band gap in Al-defect system and Ti-doped-Al-defect system is 6.34 and 6.29 eV, respectively. Therefore, in both the cases, the calculated band gap is more than in the pure system.

The total charge density of the B-defect system and Ti-doped-B-defect system is presented in Figure S1(d-e) in Supplementary Information. The TDOS and pDOS of B-defect system and Ti-doped B-defect system are plotted in Figure 6(c-d). In the B-defect system, the valence band edge is stabilized by (2.88 eV) and destabilized by 0.17 eV with respect to the B *2s* orbital in B-defect system and Ti-doped-B-defect system, respectively. The absence of B orbitals also reflects in the band gap of these two systems. In both cases, the band gap increases compared to their parent system. The band gap in the B-defect system is 6.32 eV whereas in the Ti-doped defect system is 6.25 eV.

4. Conclusions

The electronic, thermodynamical and molecular dehydrogenation property of the pure and Ti-doped $Al(BH_4)_3$ systems were investigated using density functional theory. The Ti-doped $Al(BH_4)_3$ system was studied to

improve the dehydrogenation property of the $Al(BH_4)_3$ system, as $Ti(BH_4)_3$ has excellent dehydrogenation property though thermodynamically unstable. To our surprise, such doping not only improved the dehydrogenation property but also their thermodynamic stability. We found that Ti interacts strongly with the BH_4 unit, which weakens the B-H bond strength and improves the dehydrogenation property. Interestingly, Ti doping at the Al site of $Al(BH_4)_3$ is thermodynamically favourable for even higher doping concentration (8.33%). The Al/B-defect formation was studied on the pure and doped aluminium borohydride system to understand the role of defects towards the dehydrogenation property. Such Al/B-defect formation is more favourable on the Ti-doped system than in pure system. Our study shows that Al/B-defect system and Ti-doped-Al/B-defect system improve the overall molecular dehydrogenation property of the $Al(BH_4)_3$ system and thus, a promising dopant for the borohydride systems. Among all the systems, we found that B-defect-$Al(BH_4)_3$ system has best dehydrogenation property. We believe our findings will encourage the experimentalists to look into the role of Ti in metal borohydride systems to improve their dehydrogenation property for the hydrogen-based fuels.

Supplementary Information (SI)

Total electron density of Ti doped $Al(BH_4)_3$ (Figure S1), partial DOS of all the hydrogens (Figure S2), Wyckoff positions of pure $Al(BH_4)_3$ (Table S1), and Bader charges of pure and Ti doped $Al(BH_4)_3$ systems (Table S2) are given in Supplementary Information related to this article which is available at www.ias.ac.in/chemsci.

Acknowledgments

We thank IIT Indore for the lab and computing facilities. This work is supported by DST-SERB (EMR/2015/002057), New Delhi. IC, AM, and KSR thank MHRD, CSIR and UGC for the research fellowship.

References

1. Chu S and Majumdar A 2012 *Nature* **488** 294
2. Dresselhaus M S and Thomas I L 2001 *Nature* **414** 332
3. Jena P 2011 *J. Phys. Chem. Lett.* **2** 206
4. Eberle U, Felderhoff M and Schüth F 2009 *Angew. Chem.* **48** 6608
5. http://energy.gov/sites/prod/files/2015/05/f22/fcto_targets_onboard_hydro_storage_explanation.pdf (Web release date May, 2015)
6. Soloveichik G, Her J H, Stephenes P W, Gao Y, Rijssenbeek J, Andrus M and Zhao J C 2008 *Inorg. Chem.* **47** 4290
7. Kojima Y, Suzuki K, Fukumoto K, Sasaki M, Yamamoto T, Kawai Y and Hayashi H 2002 *Int. J. Hydrogen Energy* **10** 1029
8. Hua D, Hanxi Y, Xinping A and Chuansin C 2003 *Int. J. Hydrogen Energy* **10** 1095
9. Kim J, Lee H, Han S, Kim H, Song M and Lee J 2004 *Int. J. Hydrogen Energy* **3** 263
10. Matsunaga T, Buchter F, Miwa K, Towata S, Orimo S and Zuttel A 2008 *Renewable Energy* **33** 193
11. Nakamori Y, Li H-W, Matsuo M, Miwa K, Towata S and Orimo S 2008 *J. Phys. Chem. Solids* **69** 2292
12. Ćerny R, Severa G, Ravnsbæk D B, Filinchuk Y, D'Anna V, Hagemann H, Haase D, Jensen C M and Jensen T R 2010 *J. Phys. Chem. C* **114** 1357
13. Bardají E G, Zhao-Karger Z, Boucharat N, Nale A, Michiel J, Setten V, Lohstroh W, Róhm E, Catti M and Fichtner M 2011 *J. Phys. Chem. C* **115** 6095
14. Semenenko K N, Kravchenko O V and Lobkovskii E B 1972 *J. Struct. Chem.* **13** 508
15. Miwa K, Ohba N, Towata S, Nakamori Y, Zuttel A and Orimo S 2007 *J. Alloys Compd.* **446-447** 310
16. Ravnsbæk D, Sørensen L, Filinchuk Y, Bwsenbacher F and Jensen T 2012 *Angew. Chem.* **124** 3642
17. Nakamori Y, Miwa K, Ninomiya A, Ohba N, Towata S, Zuttel A and Orimo S 2006 *Phys. Rev. B: Condens. Matter* **74** 45126
18. Aldridge S, Blake A J, Downs A J, Gould R O, Parsons S and Pulham C R 1997 *J. Chem. Soc. Dalton Trans.* **6** 1007
19. Hoekstra H R and Katz J J 1949 *J. Am. Chem. Soc.* **71** 2488
20. Callini E, Borgschulte A, Hugelshofer C, Ramirez-Cuesta A and Züttel A 2014 *J. Phys. Chem. C* **118** 77
21. Yuan F, Gu Q, Chen X, Tan Y, Guo Y and Yu X 2012 *Chem. Mater.* **24** 3370
22. Chu H, Qiu S, Zou Y, Xiang C, Zhang H and Xu F 2015 *J. Phys. Chem. C* **119** 913
23. Zhang Z G, Wang H, Liu J W and Zhu M 2013 *Thermochim. Acta* **560** 82
24. Ding X-L, Yuan X, Jia C and Ma Z-F 2010 *Int. J. Hydrogen Energy* **35** 11077
25. Puszkiel J A and Gennari F C 2009 *Scr. Mater.* **60** 667
26. Patel N, Fernandes R and Miotello A 2010 *J. Catal.* **271** 315
27. Liu Y, Zhou J and Jena P 2015 *J. Phys. Chem. C* **119** 11056
28. Yu X B, Grant D M and Walker G S 2008 *J. Phys. Chem. C* **112** 11059
29. Pozzo M and Alfe D 2011 *Int. J. Hydrogen Energy* **36** 15632
30. Shi B, Song Y, Dai J H and Yu H Z 2012 *J. Phys. Chem. C* **116** 12001
31. Song Y, Dai J H, Li C G and Yang R 2009 *J. Phys. Chem. C* **113** 10215
32. Song Y, Dai J H, Li C G and Yang R 2010 *Phys. Chem. Chem. Phys.* **12** 10942
33. Chaudhuri S, Graetz J, Ignatov A, Reilly J J and Muckerman J T 2006 *J. Am. Chem. Soc.* **128** 11404
34. Liu X, McGrady G S, Langmi H W and Jensen C M 2009 *J. Am. Chem. Soc.* **131** 5032
35. Jensen C, Zidan R, Mariels N, Hee1 A and Hagen C 1999 *Int. J. Hydrogen Energy* **5** 461

36. Li S, Jena P and Ahuja R 2006 *Phys. Rev. B: Condens. Matter* **73** 214107
37. Mao J, Guo Z, Nevirkovets I P, Liu H K and Dou S X 2012 *J. Phys. Chem. C* **116** 1596
38. Song Y, Guo Z X and Yang R 2004 *Phys. Rev. B: Condens. Matter* **69** 094205
39. Kresse G and Joubert D 1999 *Phys. Rev. B: Condens. Matter* **59** 1758
40. Perdew J P, Chevary J A, Vosko S H, Jackson K A, Pederson M R, Singh D J and Fiolhais C 1992 *Phys. Rev. B: Condens. Matter* **46** 6671
41. Blochl P E 1994 *Phys. Rev. B: Condens. Matter* **50** 17953
42. Grimme S, Antony J, Ehrlich S and Krieg S 2010 *J. Chem. Phys.* **132** 154104
43. Monkhorst H J and Pack J D 1976 *Phys. Rev. B: Condens. Matter* **13** 5188
44. Ozolins V, Majzoub E H and Wolverton C 2009 *J. Am. Chem. Soc.* **131** 230
45. Larsson P, Moysés Araújo J C, Larsson A, Jena P and Ahuja R 2008 *Proc. Natl. Acad. Sci. U.S.A* **105** 8227
46. Wang K, Zhang J-G, Jiao J-S, Zhang T and Zhou Z-N 2014 *J. Phys. Chem. C* **118** 8271
47. Kresse G 2000 *Phys. Rev. B: Condens. Matter* **62** 8295
48. Bader R F W 1991 *Chem. Rev.* **91** 893
49. Henkelman G J, Arnaldsson A and Jónsson H 2006 *Comput. Mater. Sci.* **36** 354
50. Sanville E, Kenny S D, Smith R and Henkelman G 2007 *J. Comput. Chem.* **28** 899
51. Chibisov A N 2014 *Comput. Mater. Sci.* **82** 131
52. Du A J, Smith S C, Yao X D and Lu G Q 2007 *J. Phys. Chem. C* **111** 12124
53. Guo-ying Z, Gui-li L and Hui Z 2012 *Trans. Nonferrous Met. Soc. China.* **22** 1717
54. Zhang P, Xu B, Li X, Zeng Y and Meng L 2014 *Int. J. Hydrogen Energy* **39** 17144